# Numerical flow simulator for three-phase compressible flow in porous media based on a Total Differential Compatible condition

R. di Chiara Roupert[(a)*], G. Schäfer[(a)], M. Quintard[(b)], G. Chavent[(c,d)], Ph. Ackerer[(a)], J-M. Côme[(e)]

*(a) Université de Strasbourg, Laboratoire d'Hydrologie et de Géochimie de Strasbourg, CNRS UMR 7517*
*(b) Université de Toulouse, Institut de Mécanique des Fluides de Toulouse, CNRS UMR 5502*
*(c) Université Paris-Dauphine, Ceremade*
*(d) Institut National de Recherche en Informatique et Automatique – Rocquencourt*
*(e) Burgéap, Agence de Lyon, Lyon*
** dichiara@unistra.fr*

## 1 Introduction

Two different strategies are currently used to model multiphase flow in porous media [20]. Using the first approach, in the case of a DNAPL migrating in an unsaturated zone, the water-oil-gas three-phase system can be modelled by three pressure equations obtained by substituting of Darcy's velocity of each fluid phase into the individual mass balance equations. This system of pressure equations can be transformed into a pressure-saturation form by using the relationship between the capillary pressure, which is the difference between the phase pressures and the fluid saturation. The pressure of the second and third fluid phases can then be removed by expressing this pressure in terms of the saturation and pressure of the other phase. This latter approach is useful when phase disappearance occurs and saturation becomes zero. The system of partial differential equations describing a three-phase flow is highly non-linear due to the nature of the relative permeability and capillary pressure functions needed to close the system. Alternative forms of these governing flow equations have been investigated to develop better computational algorithms. This has led to the fractional flow approach, which originates from the petroleum industry. In this approach, the total fluid flow describes the individual phases as a fraction of the total flow [6]. Through the fractional flow formulation, the immiscible displacement of oil, gas and water can be expressed in terms of three coupled equations, namely, a mean pressure equation [22, 23] or global pressure equation [11] usually and two saturation equations. In this paper, a fractional three-phase flow formulation is chosen using a global pressure approach. The construction of Total Differential (TD) three-phase data is given for the implementation of the exact global pressure formulation. This global formulation reduces the coupling between the pressure and saturation equations [14]. However, the developed global pressure approach only exists for three-phase data which satisfy a TD condition. The numerical construction of TD data such as the global mobility and global capillary pressure is achieved using $C^0$ and $C^1$ finite elements to solve respectively an harmonic and a biharmonic problem [13, 14, 15]. Corresponding TD three-phase data are given to solve fractional flow equations using an IMPES approach. Each saturation equation is treated by operator splitting i.e. a mixed-hybrid finite element method for diffusion terms while discontinuous finite element deals with advection terms. The developed model is tested on the Five-spot water flood problem and compared with some numerical solutions.

## 2 Governing equations for three-phase flow in porous media

Following notations will be used for three fluid phases: $j$=1 stands for water, $j$=2 stands for oil and $j$=3 stands for gas. We recall here the equations associated with the reformulated three-phase flow using the TD condition.

*2.1 Global pressure equation*

Classical numerical solutions using a fractional flow formulation lead to a " pressure equation" with respect to one of the three phase pressures, for example the oil pressure , and two "saturation" equations with respect to and . Let us introduce the *volum factor* evaluated at a given global pressure level $p$ satisfying $p_1 \le p \le p_3$ :

$$B_j(p) = \rho_j(p) / \rho_j(p^0) , \quad (1)$$

for $j$=1,2,3 with the reference pressure and the density of the fluid phase $j$. For a saturation distribution, *Muskat's law* is currently used to represent the *volumetric flow vector* for fluid phase $j$ at the REV scale [3]:

$$\phi_j = -d_j(P_j) kr_j(S) K.(\nabla P_j - \rho_j(P_j) g \nabla Z) , \quad (2)$$

where $d_j$, $kr_j$, $\mu_j$, $Z$, $g$ and $K$ are respectively the relative phase mobility, the relative phase permeability, the dynamic viscosity, the depth, the gravity constant and the absolute permeability. Summing up mass balance equations for $j$=1,2,3 leads to the global pressure equation:

$$\frac{\partial}{\partial t}(\varphi \sum_{j=1}^{3} B_j S_j) + \nabla.(q) = \sum_{j=1}^{3} Q_j , \quad (3)$$

where φ is the porosity, is the source/sink term of *jth* phase. The global pressure $P$ is defined as related to the oil pressure and saturation $S = (S_1, S_3)$ by:

$$P = P_2 + P_c^g(S, P) , \quad (4)$$

where $P_c^g$ is a *global capillary* function. This function has to satisfy a "*total differential"* (TD) condition [11, 13]. When this condition holds, the *volumetric flow rate q* is re-written in a *Darcy law* form:

$$q = -dK.(\omega \nabla P - \bar{\rho} g \nabla Z) , \quad (5)$$

with $\omega = 1 - \partial P_c^g / \partial p$ , $d$, $f_1$, $f_3$, $\bar{\rho}$ are respectively the *compressibility factor*, the global mobility, the water and gas fractional flows and the global density expressed as function of the *pressure level p* :

$$\begin{aligned} & d(s, p = kr_1(s) d_1(p) + kr_2(s) d_2(p) + kr_3(s) d_3(p) \\ & f_j(s, p) = kr_j(s) d_j(p) / d(s, p), \; j = 1,2,3 \\ & \bar{\rho} = \sum_{j=1}^{3} \rho_j f_j \\ & \sum_{j=1}^{3} f_j = 1 \end{aligned} \quad (6)$$

We assume that φ and $K$ are only functions of space. In the *exact global pressure* formulation, phase pressure levels are used. Based on the capillary pressure conventions, relative phase mobilities are written such as $d_1 = d_1(p_2 + P_c^{12}(s_1))$ , $d_2 = d_2(p_2)$ , $d_3 = d_3(p_2 + P_c^{32}(s_3))$ , and similarly for $\rho_1, \rho_2, \rho_3$ . Here, $P_c^{12}$ is the water-oil capillary pressure function and $P_c^{32}$ is the gas-oil capillary pressure function.

*2.2 Water and gas saturation equations*

The corresponding water and gas saturation equation satisfying the *TD condition* can be written for $j$=1,3 :

$$\begin{aligned} & \varphi \frac{\partial}{\partial t}(B_j S_j) + \nabla.(q_j) = Q_j , \\ & q_j = \omega^{-1} f_j q - d f_j K.(\nabla P_c^{jg} + g(\Delta \rho_j + \bar{\rho} \frac{1-\omega}{\omega}) \nabla Z), \end{aligned} \quad (7)$$

with $q_j$ the *jth* phase volumetric flow rate and $\Delta\rho_j=(1-f_j)(\rho_2-\rho_j)+f_{j+1}(\rho_{j+1}-\rho_2)$ . We introduced the following notation $P_c^{jg}=P_c^{j2}-P_c^g$ . For three-phase flows modelling, one can see that some secondary variables such as fractional flows, global mobility *d*, global capillary function $P_c^g$ need to be quantified in order to satisfy the TD condition [13] and thus to solve three-phase reformulated flow. In the next section, we give a short description of the practical approach used to interpolate TD three-phase data on the water-oil-gas diagram *T*.

## 3 Description of the TD-interpolation approach and required data

In the *exact global pressure* formulation, *d*, $f_1$, $f_2$, $f_3$, $\bar{\rho}$ are functions expressed from the *oil pressure level* (see equation (4)). Initial two-phase flow data are set on water-oil side, gas-oil side and water-gas side $T^{13}$ (see Figure 1). We solve first *Non-Linear Initial Value Problems* on the three two-phase sides of the ternary diagram *T* with an *Ordinary Differential Equation (ODE) Solver* [18, 26]. Therefore, global capillary function is calculated on the three two-phase boundaries. In order to satisfy the TD condition on the boundaries, the global capillary function needs to be slightly modified on the gas-oil side to provide an exact matching value at the gas vertex [13, 18]. Then the three two-phase global mobilities *d* on boundaries are computed in (6) with *P* replaced by $P_j$. The global mobility is then obtained from previous Dirichlet boundaries condition by solving an harmonic equation on *T* by means of $C^0$ piecewise linear finite elements. In the last step the global capillary pressure is extended to the whole ternary diagram *T*. It is necessary to complete the Dirichlet conditions by Neumann conditions (see Figure 1).

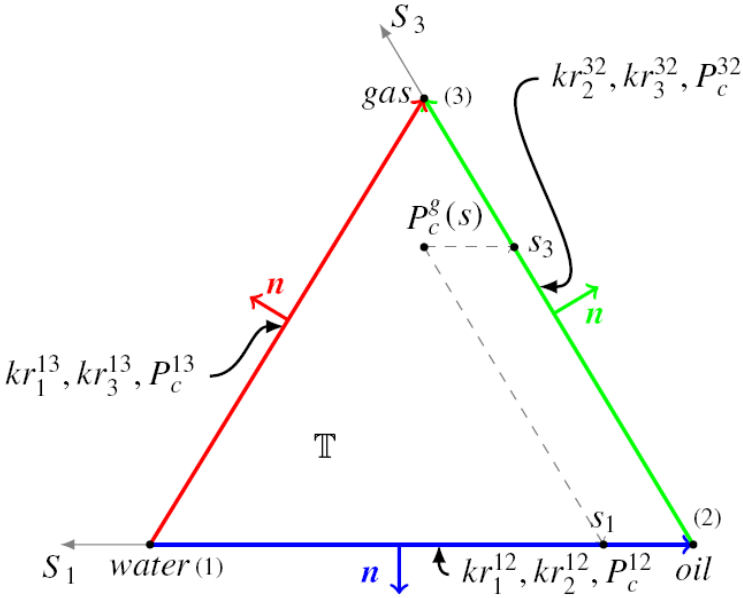


**Figure 1 : Ternary diagram T with two-phase required data.**

A biharmonic equation over *T* is needed to provide a continuous global pressure field. It is solved by a $C^1$ *Hsieh-Clough-Tocher* finite element method [5, 16], which ensure that the fractional flows derived from $P_c^g$ are continuous over the ternary diagram. For each fluid phase, the corresponding fractional flow is then derived for *i*=1,3 using:

$$f_i(s,p)=(\partial P_c^g/\partial s_i(s,p))/(dP_c^{i2}/ds_i(s_i)) \qquad (10)$$

with oil fractional flow given by the closure relation . The global mobility *d*(*s*,*p*), fractional flows $f_j(s,p)$ and global capillary function $P_c^g(s,p)$ are known as secondary variables and allow to solve global pressure equation and saturation equations.

## 4 Numerical resolution of the pressure and saturation equation

An IMPES scheme is used and involves the sequential solution of the pressure equation and saturation equation. Time Operator splitting is used to solve transport-like saturation equation. While the global pressure equation reformulated in a diffusive form is fully implicitly formulated, the explicit form is used for the advective part of the saturation equation under the Courant criterion. The diffusive terme is solved using mixed-finite element formulation.

*4.1 Mixed-Finite Element method.* A mixed-hybrid method is applied to the global pressure equation (3). The pressure equation can be split into two equations, one for the global flux and another one for the mass balance equation which is :

$$\varphi B_3^{'} S_3 \omega \frac{\partial P}{\partial t} + \varphi B_3^{'} S_3 \omega \frac{\partial P_c^{32}}{\partial t} + \varphi (B_3 - 1) \frac{\partial S_3}{\partial t} + \nabla . (q) = Q_t \tag{11}$$

with $B_3^{'} = \partial B_3 / \partial P_3$ . One remarks that for an incompressible two-phase flow, i.e. $\omega = 1$ and $B_3 = 1$ , the resulting two equations can be re-written in a simplified form such as:

$$\begin{aligned} &\nabla . (q) = Q_t \\ &q = d\omega K \left( \nabla P - \Lambda_\rho \nabla z \right) \end{aligned} \tag{12}$$

The weak formulation of (12) is performed with test functions using lowest order Raviart-Thomas space for an element *E* when represents the so-called mixed finite element formulation. Applying the incompressibility condition, the discretized form of the variational equations is then

$$\begin{aligned} &\sum_j Q_{Ej} \underbrace{\int_E \frac{1}{\omega_E d_E} w_i . K^{-1} w_j \, dE}_{=B_{ij}} = P_E \underbrace{\int_E \nabla . w_i \, dE}_{=1} - \sum_j TP_{Ej} \underbrace{\int_{Ej} w_i . n_{Ej} \, dEj}_{=\delta_{ij}} + \Lambda_{\rho E} \underbrace{\int_E \nabla z . w_i \, dE}_{=G_{Ei}}, \\ &\sum_j Q_{Ej} \int_E \nabla . w_i \, dE = |E| Q_{t,E} . \end{aligned} \tag{13}$$

The continuity of fluxes across element edges is applied. This means the $Q_{Ej}$ expressions in (13) are isolated and substituted in the discretized element balance equations. The element global pressure $P_E$ are extracted in the element balance equation and substituted in the flux continuity equations. Thus global pressure and fluxes are eliminated and the resulting mixed-hybrid system has only the Lagrange multipliers $TP_{Ej}$ i.e. the edge global pressure. The corresponding system matrix is positive definite and solved using a conjugate gradient method. Taking into account compressibility effect and neglecting capillary effects in the variational term, the weak formulation of the mass balance equation (11) gives an element mid-point expression of the global pressure field is :

$$P_E^{n+1} = \frac{\Delta t}{\varphi |E| B_3^{'} \omega + \alpha_E \Delta t} \left( \frac{\varphi |E| B_3^{'} \omega}{\Delta t} P_E^n + \frac{\varphi (1 - B_3)}{\Delta t} \left( S_{3,E}^{n+1} - S_{3,E}^n \right) + \sum_{ij} B_{ij}^{-1} TP_{Ej}^{n+1} - \Lambda_{\rho E} \sum_{ij} B_{ij}^{-1} G_{Ej} + |E| Q_t \right) \tag{14}$$

and $\Lambda_{\rho E} = g \bar{\rho}_E / \omega_E$ . The edge global mobilities to be used by the mixed-hybrid method are derived from the upstream saturations of the previous time step. The pressure field and the fluxes over the element edges are obtained and used in saturation equations.

*4.2 Discontinuous Galerkin Finite Element method*

The discontinuous Galerkin method is applied to deal with the advective part of saturation equations. The element saturation computed explicitly from the advective term is fully determined using a slope limiter based on the Van Leer's MUSCL limiter introduced by Chavent and Jaffré [11]. An efficient geometric approach is used for general trianglar mesh by avoiding the iterative procedure of the minimization problem [30]. The weak formulation of the advective part of balance equation (7) is obtained using a test function $w_i$ :

$$\varphi \sum_j \frac{\partial B_l S_{l,j}^E}{\partial t} \int_E w_j w_i dE = \sum_j \int_E f_{l,j}^E q.\nabla w_i dE - \sum_j \int_{Ej} f_{l,Ej}^+ w_i.q.n_{Ej} dEj \ , \tag{15}$$

with $S_{l,j}^E$ is *j-th* degree of freedom of the *l-phase* saturation on element *E*. The three unknowns associated with the corresponding interpolations functions are then reformulated as :

$$\begin{aligned} S_{l,1}^E(t) &= \bar{S}_{h,l}^E, & w_1^E(x,y) &= 1, \\ S_{l,2}^E(t) &= \partial S_{h,l}^E / \partial x, & w_2^E(x,y) &= x - \bar{x}_E, \\ S_{l,3}^E(t) &= \partial S_{h,l}^E / \partial y, & w_3^E(x,y) &= y - \bar{y}_E, \end{aligned} \tag{16}$$

with $\bar{S}_{l,j}^E$ the average value of the *l-th* phase saturation on element *E*, and its two deviations in each space direction. The approximate solution $S_{h,l}^E$ is expressed with linear basis function $w_i$ on *E*. Assuming that $q.n_{Ej}$ is constant through the edge *Ej*, one has:

$$\int_{Ej} f_{l,Ej}^+ w_i.q.n_{Ej} dEj = \frac{Q_{Ej}}{|Ej|} \int_{Ej} f_{l,Ej}^+ w_i dEj \ , \tag{17}$$

and the upstream fractional flux $f_{l,Ej}^+$ are taken as $f_{l,Ej}$ *if* $q.n_{Ej} \geq 0$ and $f_{l,Ej'}$ *if* $q.n_{Ej} < 0$

For the explicit advection scheme, the CFL criterion has to be fullfilled for all elements of the domain. The geometric slope limiting procedure is used to avoid unphysical oscillations in the numerical solution. The saturation $\tilde{S}_{l,mi}$ at the mid-point $(x_{mi}, y_{mi})$ of edge *Ei* is obtained such as:

$$\tilde{S}_{l,mi} = \bar{S}_{h,l}^E + \partial \tilde{S}_{h,l}^E / \partial x \left( x_{mi} - \bar{x}_E \right) + \partial \tilde{S}_{h,l}^E / \partial y \left( y_{mi} - \bar{y}_E \right) . \tag{19}$$

The limiting procedure is only preformed on the two deviations in order to obtain the reconstructed deviations values $\left( \partial S_{h,l}^E / \partial x, S_{h,l}^E / \partial y \right)$. The average value $\bar{S}_{h,l}^E$ is kept unchange to preserve local mass balance.

## 5 Study case: Five spot waterflood problem in a homogeneous porous medium

The five-spot water flood problem comprises two cases and allows also to test the influence of grid orientation on the numerical results (Fig. 2). The study case assumes the flow of two immiscible and incompressible fluids in a homogeneous medium without capillarity. The numerical study deals with the displacement of a non-aqueous phase liquid (oil) by water in a square-shape domain. Similarly to the Buckley-Leverett case, there is no water initially present in the system. The domain is discretized by 16x16, 32x32 and 64x64 regular triangular elements. The first case (see Figure 2a) is called ‘diagonal grid’ case where water is injected at the lower left corner of the domain. The principal direction is diagonal to the grid. In the second case called ‘parallel grid’ case, water is injected at the lower left and upper right corner and thus allow oil leaving the domain at the upper left and lower right corner. The Todd relative permeability-saturation relationship is used with a viscosity ratio of $\mu_w / \mu_o = 4$ .

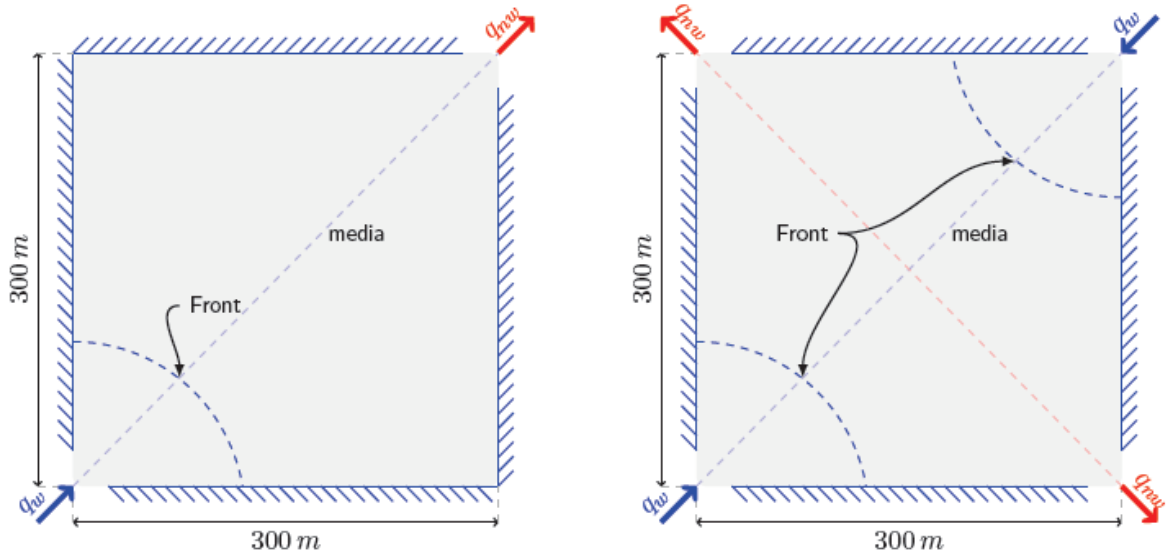


**Figure 2 : Five-spot waterflood problem: (a) diagonal grid; (b) parallel grid**

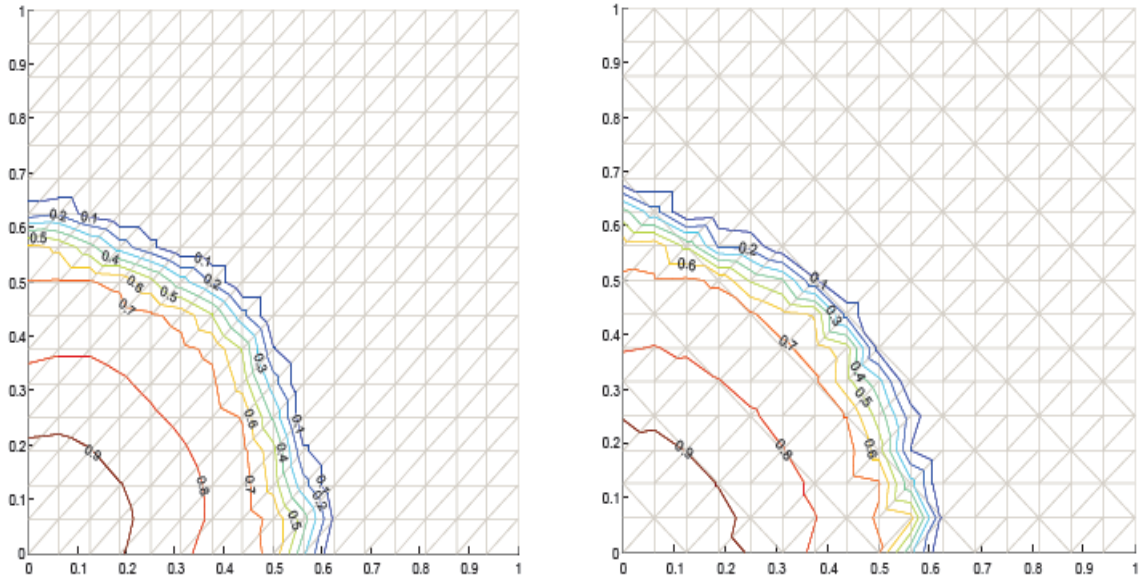

**Figure 3 : Calculated water saturation in the diagonal grid case 16x16 with two different grid orientation : (a) diagonal (left), (b) alternate (right) after 200 days**

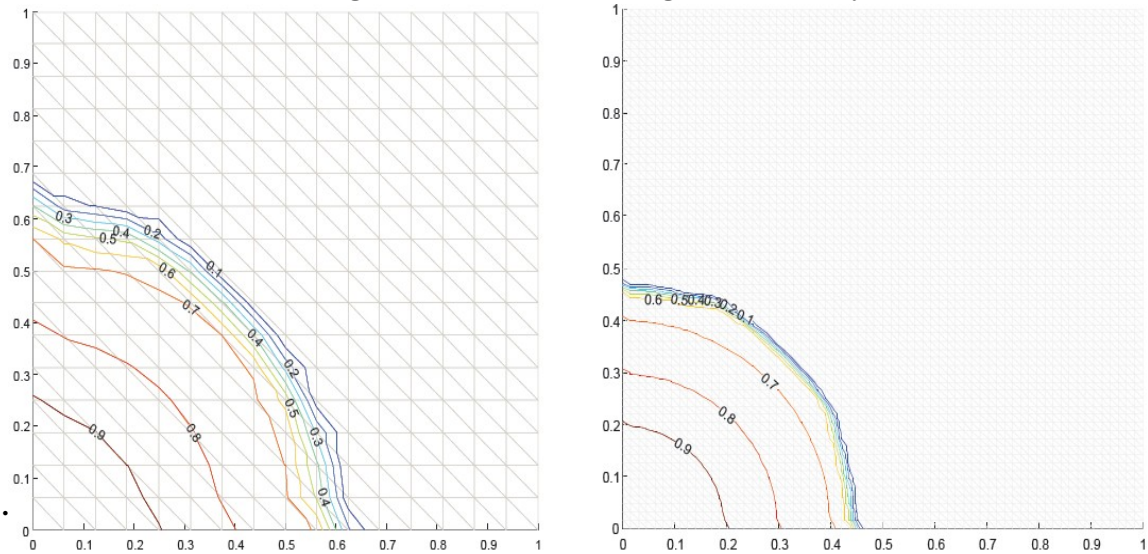

**Figure 4 : Calculated water saturation in the diagonal grid case 16x16 (left) and 64x64 grid case (right) with an opposite diagonal orientation after 200 days.**

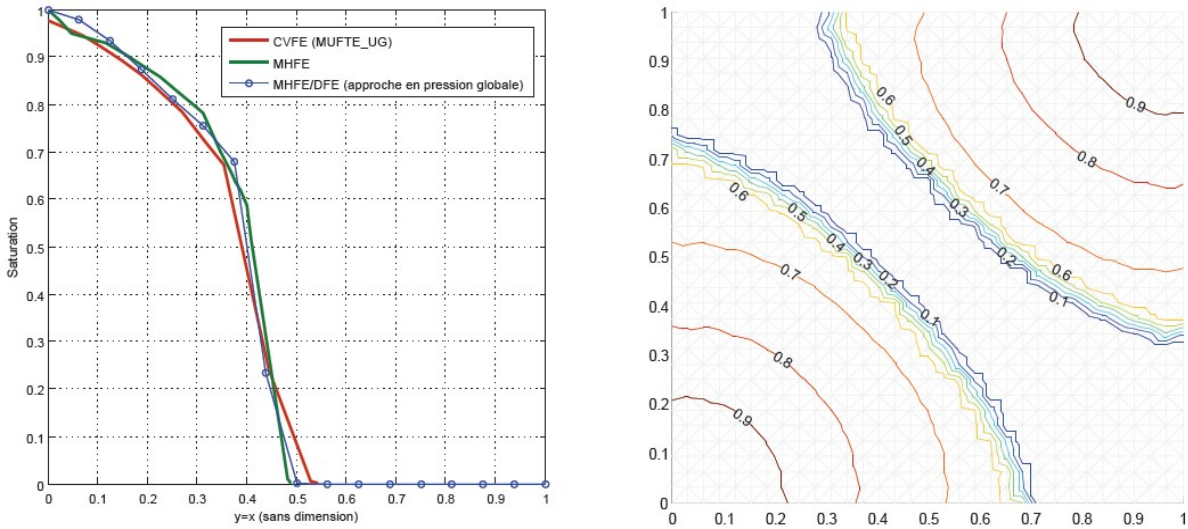


**Figure 5 : Cross-section of the water saturation profile along y=x in the diagonal grid case 16x16 (left) compared with MUFTE_UG and solution in Helmig, 1997 [20], parallel case for 32x32 grid after 200 days.**

Figures 3, 4 and 5 show the numerical results obtained. The reformulated global pressure formulation combined with the chosen numerical schemes does not have significant numerical transverse diffusion due to grid orientation. For both parallel and diagonal grid cases, the water saturation front propagates faster along boundaries of the square than in direction of the diagonal. For a fine 64x64 grid, the influence of grid orientation disappears and we get a undeformed quarter-circle with a good sharp-front of the water saturation. A numerical comparison with the 16x16 solution given by Helmig, 1997 [20] and with MUFTE_UG is shown in figure 5. Our mixed hybrid-discontinuous finite element (MHFE/DFE) used for the global pressure formulation converges toward the two other numerical solutions.

## 6 Conclusion

The reformulation of the fractional flow equation for three-phase flow modelling using a TD condition and the re-writing of three-phase compressible flow equations in a more suitable fractional form (see (5) and (7)) were presented. A first $C^0/C^1$ parametrization was performed to obtain TD three-phase secondary variables used in the flow simulator. Then numerical schemes such as mixed-hybrid and discontinuous finite element were used to discretize both the global pressure and saturation equation. First numerical results obtained are presented in the case of a two-phase flow problem. Further research work will focus on testing of the developed flow simulator on more complex situations.

## References

[1] B. Amaziane, M. Jurak, A new formulation of immiscible compressible two-phase flow in porous media, C. R. Mécanique 336 (2008) 600–605.

[2] S.N. Antoncev, V.N. Monahov, Three-dimensional problems of time-dependant two-phase filtration in non-homogeneous anisotropic porous media, Soviet Math. Doklady 19 (1978) 1354–1358.

[3] J. Bear, Dynamics of Fluids in Porous Media, Elsevier, New York, 1972.

[4] H. Benremita, G. Schäfer, Transfert du trichloréthylène en milieu poreux à partir d'un panache de vapeurs, C. R. Mécanique 331 (2003) 835–842.

[5] M. Bernadou, K. Hassan, Basis functions for general Hsieh-Clough-Tocher triangles complete or reduced, Inria Research Report RR-5, 1980.

[6] P. Binning, M.A. Celia, Practical implementation of the fractional flow approach to multi-phase flow simulation, Adv. Water Resour 22 (5) (1999) 461–478.

[7] M. Bohy, G. Schäfer, O. Razakarisoa, Caractérisation de zones sources de DNAPL à l'aide de traceurs bisolubles : mise en évidence d'une cinétique de partage, C. R. Geoscience 336 (2004) 799–806.
[8] M. Bohy, L. Dridi, G. Schäfer, O. Razakarisoa, Transport of a mixture of chlorinated solvent vapors in the vadose zone of a sandy aquifer, Vadose Zone Journal 5 (2006) 539–553.
[9] R. Byrd, P. Lu, J. Nocedal, C. Zhu, A limited memory algorithm for bound constrained optimization, Computer Science Department, University of Colorado at Boulder NAM-08, 1994.
[10] G. Chavent, G. Salzano, Un algorithme pour la détermination de perméabilités relatives triphasiques satisfaisant une condition de différentielle totale, Inria Research Report RR-0355, 1985.
[11] G. Chavent, J. Jaffré, Mathematicals Models and Finite Elements fo Reservoir Simulation, North-Holland, Amsterdam, 1986.
[12] G. Chavent, R. di Chiara Roupert, G. Schäfer, A Fully Equivalent Global Pressure Formulation for Three-Phase Compressible Flows, Conference Scaling'Up 08, Dubrovnik, October 13-16 2008.
[13] G. Chavent, A Fully Equivalent Global Pressure Formulation for Three-Phase Compressible Flow, Applicable Analysis 88 (10) (2009) 1527–1541
[14] Z. Chen, R. Ewing, Comparison of Various Formulations of Three-Phase Flows in Porous Media, Journal of Computational Physics 132 (1997) 362–373.
[15] Z. Chen, Finite Element Methods and Their Applications, Scientific Computation, Springer, Berlin, 2005.
[16] R.W. Clough, J.L. Tocher, Finite element stiffness matrices for analysis of plate bending. in Proceedings of the Conference on Matrix Methods in Structural Mechanics, Wright Patterson A.F.B, Ohio, USA, 1965.
[17] R.M. Cohen, J.W. Mercer, DNAPL site evaluation. In: Smoley, C.K. (Ed.), CRC Press, Florida, USA, 1993.
[18] R. di Chiara. Développement d'un code de calcul multiphasique multiconstituants. PhD thesis, Université de Strasbourg, France, 2009.
[19] L. Dridi, I. Pollet, O. Razakarisoa, G. Schäfer. Characterisation of a DNAPL source zone in a porous aquifer using the Partitioning Interwell Tracer Test and an inverse modelling approach, Journal of Contaminant Hydrology (2009) doi: 10.1016/j.jconhyd.2009.03.003.
[20] R. Helmig, Multiphase flow and transport processes in the subsurface. A contribution to the modeling of hydrosystems. Springer (Environmental Engineering), 1997.
[21] S. Jégou, Estimation des perméabilités relatives dans des expériences de déplacements triphasiques en milieu poreux. Thése, Université Paris IX Dauphine, France, 1997.
[22] D. Nayagum, G. Schäfer, R. Mose, Approximation par les éléments finis mixtes d'une équation de diffusion non linéaire modélisant un écoulement diphasique en milieu poreux, C.R. Acad. Sci Paris 239 (2001) 87–90.
[23] D. Nayagum, G. Schäfer, R. Mose, Modeling two-phase incompressible flow in porous media using mixed hybrid and discontinuous finite elements, Computational Geosciences 8 (2004) 49–73.
[24] F. Nex, G. Schäfer, J.-M. Côme, T.M. Vogel, Une approche innovante pour modéliser la biodégradation des composés organo-chlorés volatils en aquifères poreux, C.R. Geoscience 338 (2006) 287–306.
[25] J.C. Parker, R.J. Lenhard, T. Kuppusami, A parametric model for constitutive properties governing multiphase flow in porous media, Water Resour. Res. 23 (1987) 618–624
[26] A. Quarteroni, R. Sacco, F. Saleri, Méthodes Numériques - Algorithme, analyse et applications, Springer, Italia, 2007.

[27] A. Sinke, I. Le Hecho, Monitored natural attenuation: review of existing guidelines and protocols, TNO-Nicole report, Apeldoorn, The Netherlands, 1999.
[28] H.M. Stone, Probability model for estimating three-phase relative permeabilitiy, Journal of Petroleum Technology 22 (1970) 214–218
[29] M.T. Van Genuchten, A closed-form equation for predicting the hydraulic conductivity of unsaturated soils, Soil Sci. So. Am. J. 44 (1980) 892–989
[30] A. Younes, P. Ackerer, and M. Fahs. An efficient geometric approach to solve the slope limiting problem with discontinuous galerkin method on unstructured triangles. Communication in numerical methods in engineering, 2009.